that leads to the matrices in Eq. (6)

$$A=\begin{bmatrix} A_p & 0 & 0 \\ A_m & 0 & B_m \\ 0 & 0 & D \end{bmatrix} \quad B=\begin{bmatrix} B_p \\ 0 \\ 0 \end{bmatrix} \tag{18}$$

and respectively in Eq. (7):

$$Q_o=\begin{bmatrix} Q & -Q & 0 \\ -Q & Q & 0 \\ 0 & 0 & 0 \end{bmatrix} \qquad R \text{ unchanged} \tag{19}$$

The tilde matrices are then written:

$$\tilde{R}=R+B_p^T Q B_p \tag{20}$$

$$\tilde{Q}_o=\begin{bmatrix} \tilde{Q} & -\tilde{A} & 0 \\ -\tilde{Q} & \tilde{Q} & 0 \\ 0 & 0 & 0 \end{bmatrix} \quad \text{with } \tilde{Q}=Q-QB_p\tilde{R}^{-1}B_p^T Q \tag{21}$$

$$A=\begin{bmatrix} \tilde{A}_p & 0 & B\tilde{R}^{-1}B_p^T Q B_m \\ A_m & 0 & B_m \\ 0 & 0 & D \end{bmatrix}$$

$$\text{with } \tilde{A}_p=A_p-B_p\tilde{R}^{-1}B_p^T Q(A_p-A_m) \tag{22}$$

If the matrix $\boldsymbol{P}$ in the Riccati equation is partitioned into 9 submatrices, the relation (15) yields 6 independant equations because of the symmetry of $\boldsymbol{P}$:

$$\dot{P}_{11}=-P_{11}\tilde{A}_p-P_{12}A_m-\tilde{A}_p^T P_{11}-A_m^T P_{12}$$
$$+P_{11}B_p\tilde{R}^{-1}B_p^T P_{11}-(A_p-A_m)^T\tilde{Q}(A_p-A_m) \tag{23a}$$

$$\dot{P}_{12}=-\tilde{A}_p^T P_{12}-A_m^T P_{22}+P_{11}B_p\tilde{R}^{-1}B_p^T P_{12} \tag{23b}$$

$$\dot{P}_{13}=-P_{11}B_p\tilde{R}^{-1}B_p^T QB_m-P_{12}B_m-P_{13}D-\tilde{A}_p^T P_{13}$$
$$-A_m^T P_{23}+P_{11}B_p\tilde{R}^{-1}B_p^T P_{13}+(A_p-A_m)^T\tilde{Q}B_m \tag{23c}$$

$$\dot{P}_{22}=P_{12}B_p\tilde{R}^{-1}B_p^T P_{12} \tag{23d}$$

$$\dot{P}_{23}=-P_{12}B_p\tilde{R}^{-1}B_p^T QB_m-P_{22}B_m$$
$$-P_{23}D+P_{12}B_p\tilde{R}^{-1}B_p^T P_{13} \tag{23e}$$

$$\dot{P}_{33}=-P_{13}B_p\tilde{R}^{-1}B_p^T QB_m-P_{23}B_m-P_{33}D$$
$$-(B_p\tilde{R}^{-1}B_p^T QB_m)^T P_{13}-B_m^T P_{23}$$
$$-D^T P_{33}+P_{13}B_p\tilde{R}^{-1}B_p^T P_{13}-B_m^T\tilde{Q}B_m \tag{23f}$$

From the boundary value $P(T)=0$, it follows successively $P_{12}(t)\equiv 0$, $P_{22}(t)\equiv 0$ and $P_{23}\equiv 0$. Because of the particular from of B in Eq. (18), only the first row of $\boldsymbol{P}$ is involved in the control law (16), that can be written:

$$u_p^*=-\tilde{R}^{-1}B_p^T\{[P_{11}+Q(A_p-A_m)]x_p+$$
$$[P_{13}-QB_m]u_m\} \tag{24}$$

The result $P_{12}(t)\equiv 0$ is consistent with the fact that the vector x_d is fictitious and could not play a role in the real control algorithm. Both other matrices are then solutions of the relations (23a) and (23c) that read after simplification:

$$\dot{P}_{11}=-P_{11}\tilde{A}_p-\tilde{A}_p^T P_{11}+P_{11}B_p\tilde{R}^{-1}B_p^T P_{11}$$
$$-(A_p-A_m)^T\tilde{Q}(A_p-A_m) \tag{25a}$$

$$\dot{P}_{13}=-P_{11}B_p\tilde{R}^{-1}B_p^T QB_m-P_{13}D-\tilde{A}_p^T P_{13}$$
$$+P_{11}B_p\tilde{R}^{-1}B_p^T P_{13}+(A_p-A_m)^T\tilde{Q}B_m \tag{25b}$$

with $P_{11}(T)=P_{13}(T)=0$ and the matrices $\tilde{R}$, $\tilde{Q}$ and $\tilde{A}_p$ given in Eqs. (20-22).

Equations (24) and (25) represent the solution to the problem of Eqs. (1-5) for optimal following of a forced model. Previously known equations for the free implicit model[1,5,6] are obtained simultaneously with D, B_m, and P_{13} equal zero.

Conclusions

Kriechbaum and Stineman[9] have recently published similar results, obtained by discrete dynamic programing and letting the time interval approach zero. They also assume that model inputs are slowly varying and can be considered as constant over some time. A detailed comparison shows that their expressions [Eqs. (21-26)] may be obtained from the relations (25) above, with $D\equiv 0$ in Eq. (4). It is thus felt that the present paper, while matching the theoretical line of previous references, offers some more generality than Ref. 9 in allowing time-varying model inputs.

References

[1] Tyler, J. S., "The Characteristics of Model-Following Systems as Synthesized by Optimal Control," *IEEE Transactions on Automatic Control*, Vol. AC-9, Oct. 1964, pp. 485-498.

[2] Kalman, R. E. and Englar, T. S., "Matching Dynamics," *A User's Manual for the Automatic Synthesis Program, ASP Program C*, CR-475, June 1966, NASA.

[3] Asseo, S. J., "Application of Optimal Control to Perfect Model Following," *Journal of Aircraft*, Vol. 7, July/Aug. 1970, pp. 308-313.

[4] Erzberger, H., "On the Use of Algebraic Methods in the Analysis and Design of Model-Following Control Systems," TN D-4463, June 1968, NASA.

[5] Markland, C. A., "Design of Optimal and Suboptimal Stability Augmentation Systems," *AIAA Journal*, Vol. 8, April 1970, pp. 673-679.

[6] Markland, C. A., "Optimal Model-Following Control System Synthesis Techniques," *Proceedings IEEE*, Vol. 117, March 1970, pp. 623-627.

[7] Landau, I. D., "Model Reference Adaptive Systems—A Survey; MRAS—What is Possible and Why?" *Transactions of the ASME: Journal of Dynamic Systems, Measurement, and Control*, June 1972, pp. 119-132.

[8] Tiroshi, I. and Elliott, J. R., "Explicit Model Following Control Scheme Incorporating Integral Feedback," *Journal of Aircraft*, Vol. 11, June 1974, pp. 364-366.

[9] Kreichbaum, G. K.L. and Stineman, R. W., "Design of Desirable Airplane Handling Qualities via Optimal Control," *Journal of Aircraft*, Vol. 9, May 1972, pp. 365-369.

Wave Structure of Exhausts

Allen E. Fuhs*
Naval Postgraduate School, Monterey, Calif.

In a previous Note,[1] a method was suggested whereby shock diamonds could be eliminated by appropriate choice

Received April 7, 1975. The work reported herein was supported by Naval Ordnance Station, Indian Head, Md.

Index categories: Jets, Wakes and Viscid-Inviscid Flow Interation; Airbreathing Propulsion, Subsonic and Supersonic.

*Professor of Mechanical Engineering. Associate Fellow AIAA.

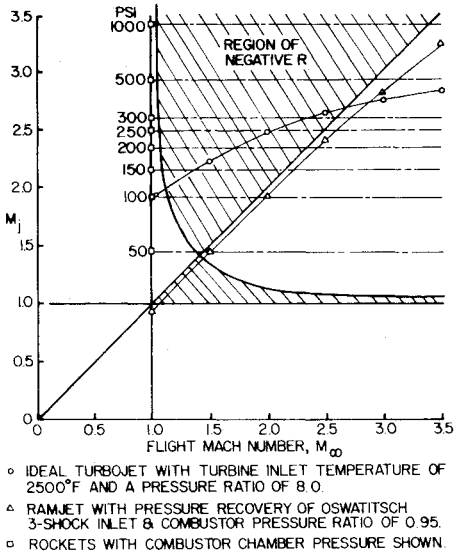

Fig. 1 Curves of M_j vs M_∞ superimposed on the map of reflection coefficient.

of exhaust Mach number. For purpose of reduced exhaust plume signature, elimination of shock diamonds is desirable. The technique is applicable to exhaust from ramjets, rockets, or aircraft gas turbines.

It is of interest to examine the jet Mach number M_j for ramjets, rockets, and gas turbines as a function of Mach number M_∞. Figure 1 shows curves of M_j as a function of M_∞ superimposed on a map of reflection coefficient.

For a rocket, the value of M_j is independent of M_∞. Consequently, the curves are straight lines at constant M_j. Assuming expansion of an ideal gas, the value of M_j is determined by the ratio of heat capacities γ and the ratio of chamber pressure to ambient pressure. Chamber pressures are given in Fig. 1; the rocket is assumed to be at sea level and to have propellants yielding $\gamma = 1.4$. A curve for constant chamber pressure moves upward with increasing altitude. Shock diamonds should be absent for a narrow range of M_∞ near transonic and high supersonic values of M_∞. For a more precise definition of the values of M_∞ with no shock diamonds, it is obvious that Fig. 1 should be recalculated for values of γ more appropriate for rockets; the trends shown by Fig. 1 would be correct at other values of γ.

For an ideal ramjet, $M_j = M_\infty$. When losses are taken into account, the values of $M_j < M_\infty$. The ramjet curve in Fig. 1 is below the diagonal $M_j = M_\infty$. For the case illustrated, there are shock diamonds for $1.0 < M_\infty < 1.4$. For $M_\infty > 1.4$, the diamonds are absent.

A curve of M_j vs M_∞ was calculated for an ideal turbojet with a compressor having a fixed pressure ratio of 8.0. For $M_\infty > 2.6$ and near transonic, the shock diamonds do not occur. For an upper bound on turbine inlet temperature, the optimum compressor pressure ratio decreases as M_∞ increases; eventually the optimum blends a turbojet into a ramjet. A consequence of optimizing compressor pressure ratio with changes in M_∞ would be to lower the turbojet curve in Fig. 1. Also component inefficiencies, e.g., compressor efficiency, would tend to lower the curve.

In summary, the following conclusions can be drawn from Fig. 1. For practical rocket chamber pressures, the shock diamonds will not be eliminated except at high supersonic M_∞ and an insignificant transonic region; a ramjet should operate without shock diamonds for all M_∞ in excess of approximately 1.4; and current supersonic aircraft (e.g., F-4, F-14, F-15) should have shock diamonds whenever M_∞ exceeds unity by a slight amount. However, advanced turbojet-propelled aircraft should not have shock diamonds whenever M_∞ exceeds 2.6 or so.

References

[1] Fuhs, A. E., "Wave Structure of Exhaust from Transonic Aircraft," *Journal of Aircraft*, Vol. 8, 1971, pp. 280-281.

Technical Comments

Comment on "Advanced Technology Thrust Vectoring Exhaust Systems"

J.A.C. Kentfield*
University of Calgary, Calgary, Alberta, Canada

GILL[1] recently presented the results of a study aimed at identifying suitable thrust vectoring nozzles for the lift-cruise engine of a specific VTOL aircraft type operating a prescribed mission. Gill's remarks relating to the installational characteristics of the nozzles he considered are in general agreement with the findings of an earlier study.[2] There are, however, comments which can be made relating to the choice of two of the nozzle types considered by Gill.

For turbofans augmented in the cruise mode only (the engine type shown by Gill to be preferred for the mission he considered), the use of a slider instead of a trap door to control the downflow of a ventral nozzle appears to merit consideration. It permits the downward projection, and hence the frontal area, of the engine to be reduced, compared with that of a trap-door nozzle with fixed side plates ($V \approx 0.13$ instead of $V = 0.23$; see Fig. 11 of Gill's paper). A slide-valve controlled ventral nozzle arrangement is illustrated in Fig. 1. Lateral vanes are provided in the ventral opening in order to permit a range of vectoring, with the full engine flow passing through the ventral opening, for approximately 30° aft to about 10° ahead of vertical. The width of the opening is tailored to accommodate the influences of flow vector angle and nonuniformity of discharge coefficient as a function of slider position. With respect to the range of vectoring using only the ventral opening, the slide valve and trap-door concepts appear to be comparable.

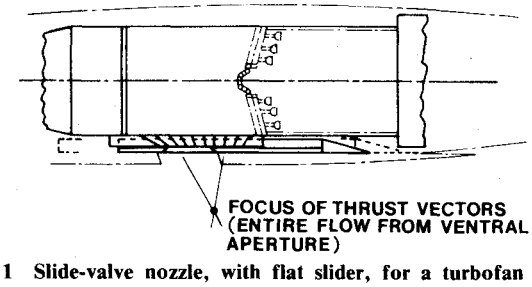

Fig. 1 Slide-valve nozzle, with flat slider, for a turbofan engine augmented in the cruise mode only.

Received January 28, 1975; revision received February 24, 1975.
Index categories: VTOL Aircraft Design; VTOL Missions and Transportation Systems; VTOL Powerplant Design and Installation.
*Associate Professor, Mechanical Engineering Department. Member AIAA.